Comparaison between three methods for determining principal stress directions from focal mechanisms inversions

Julie Maury* (maury@unistra.fr) and François Cornet*

*IPGS EOST, CNRS/UMR7516, 5 rue René Descartes, Strasbourg, France

ABSTRACT

We invert 35 focal mechanisms from the 1980 Sierentz seismic crisis (Southern Upper Rhine Graben) with three different methods to determine the principal stress directions and the principal stress magnitude aspect ratio. We compare the results and errors domains obtained with each method.

The three inversion methods yield similar results, within 10° of each other, the minimal stress direction being well constrained but the other parameters being much less well defined. Borehole Breakouts and Drilling Induced Tension Fractures help discuss the validity of the results.

INTRODUCTION

Earthquakes are a useful tool to evaluate the state of stress within the crust at depth. Several inversion methods using focal mechanisms have been developed to infer the direction of the principal stresses and their relative magnitude. They are based on different assumptions but the inversion results are often fairly similar (Hardebeck and Hauksson (2001).

We compare in this presentation results from the inversion methods proposed by Gephart and Forsyth (1984), by Michael (1984, 1987) and by Angelier (2002) in the context of the seismic crisis that occurred in Sierentz (Southern Upper Rhine Graben) in 1980.

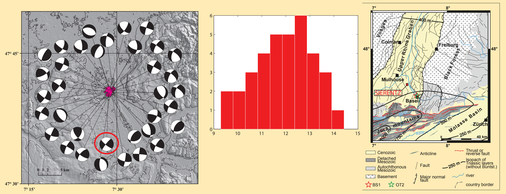

Figure 1: Left, focal mechanisms from the Sierentz sequence (courtesy of L. Dorbath). Red circle: main earthquake. Center, histogram of the depth of the 35 earthquakes. Right, location of Sierentz in th Upper Rhine graben (modified after Valley and Evans, (2009)).

DATA

July 15, 1980 an earthquake of magnitude Ml=4.9 occurred near Sierentz (Southern Upper Rhine Graben). It was followed by numerous aftershocks during the next few days (Rouland et al, 1980). 35 focal mechanisms were calculated for the aftershocks (fig. 1). Figure 2 shows their characteristics. Two preferential azimuthal directions N120°E and N210°E with steep dip are observed.

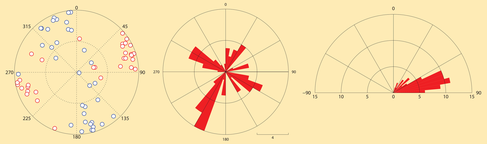

Figure 2: The first column shows P and T axes plotted in equal area projection of the lower hemisphere (blue circles=P-axes and red circles=T-axes). The next two columns show the rose diagrams of nodal planes azimuths and dips . The planes are mostly oriented N120°E and N210°E and are subvertical.

METHODS

All these methods make several assumptions:

-the medium is homogenous at the scale considered so the parameters we are looking for are constant.

-the focal mechanisms are independent from one another and representative of the stress field.

-faults slip in the direction of the resolved shear stress onto the fault plane.

The principal stress directions are defined by their azimuths and dips and their relative magnitude by the ratio R=(σ2-σ1)/(σ3-σ1).

ANGELIER (2002) (Shear Stress Slip Component Method, SSSCM):

Hypothesis:

The maximization of the shear stress slip component (SSSC) implies the maximization of the magnitude of the shear stress which implies a Tresca criterion (σ1-σ3=constant).

Principle:

We want to maximize the SSSC which is the orthogonal projection of the shear stress onto the slip vector. This method doesn't require a choice of fault plane because the SSSC value doesn't depend on the nodal plane.

Error estimation:

A fit estimator is calculated by normalizing the SSSC value with the maximal shear stress and by averaging it.

The confidence regions are then estimated using Michael (1987)'s bootstrap method.

GEPHART AND FORSYTH (1984) (Focal Mechanisms Stress Inversion, FMSI):

This is the method of Julien and Cornet (1987)'s based on Gephart and Forsyth (1984) approximate method but the final solution is computed with a gradient method.

Hypothesis:

The error is supposed to obey a normal law but a L1-norm is chosen because of the error in the choice of nodal plane (either right or wrong). L1-norm is less affected by non-normality than a L2-norm.

Principle:

For each nodal plane and for each stress tensor generated we search the minimum angle of rotation that bring the slip direction into alignment with the resolved shear stress. For a focal mechanism, the nodal plane associated with the minimal rotation is considered to be the slip plane.

Error estimation:

The sum of the minimal rotation for each focal mechanism gives a total misfit with a L1 norm. Confidence regions are estimated from the distribution of misfit values. For more details see Gephart and Forsyth (1984). Among the solutions previously determined (in the 90% domain) we optimize the solution with a least square method (Julien and Cornet (1987)).

MICHAEL (1984, 1987) (Linear Inversion Method, LSIB):

Hypothesis:

The magnitude of the shear traction is the same on all planes. It implies that the pore pressure is uniform.

The error is represented in the dataset and the dataset is not small.

Principle:

The problem is linearized because of the assumption on the magnitude of the shear stress. The problem is then solved by least squares inversion minimizing the difference between a unit vector in the slip direction and the resolved shear stress for each focal mechanism.

Error estimation:

Confidence regions are estimated using a bootstrap technique. The dataset is resampled 2000 times to simulate repeated samples of the population the data came from. In each of these resamplings a focal mechanism can be picked several times or not at all. To simulate the uncertainty on the fault plane each plane has a 50% probability of being chosen. The samples are then inverted and the 95% of the inversion results closest to the initial result define the 95% confidence region.

RESULTS

Figure 3: A: directions of the principal stresses. The outer contour defines the 95% confidence limit and the inner one the 50% confidence limit. B: variations of R=(σ1-σ2)/(σ1-σ3). In blue, the 95% and outlined in black the 50%. C: azimuths and dips selected as fault planes (in red) and all nodal planes (in blue). Since SSSCM doesn't select a fault plane we don't have the diagrams.

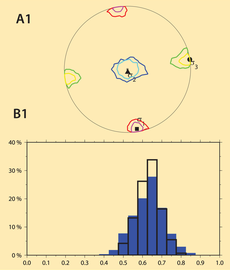

Results
*σ1=171°/4°
*σ2=174°/86°
*σ3=81°/0.2°
*r=0.64
*wm=max(Σ SSSC)/τmax/35
wm= 63%

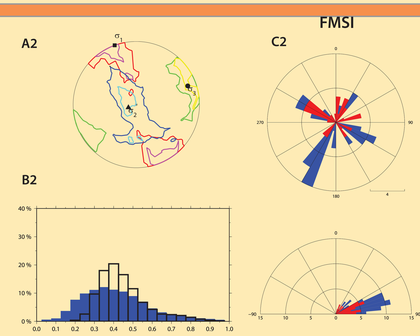

Results
*σ1=-20°/0°
*σ2=250°/79°
*σ3=70°/12°
*r=0.35
*data explained : 74%=26 events
*reduced misfit: 1.6
*50% confidence: 5.7

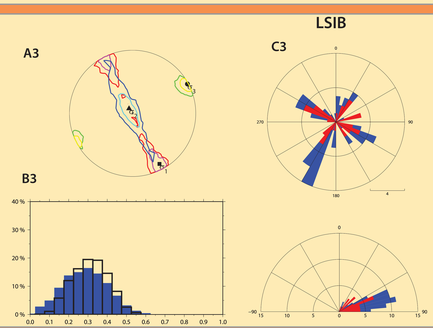

Results
*σ1=152°/8°
*σ2=-37°/82°
*σ3=62°/1°
*r=0.30
*variance: 0.11
*fit angle mean: 21

DISCUSSION

The three methods yield similar results for the orientation of the principal stress directions. However only the minimum principal stress direction is well constrained, at least for FMSI and LSIB. Further a 10° difference for the σ3 orientation is observed between the SSSCM and FMSI and LSIB and FMSI. For SSSCM, the confidence limits for the stress directions are smaller than those obtained with the other methods. Results for parameter R vary greatly between SSSCM, FMSI and LSIB and appear to be not very well constrained with FMSI (figure 3 B2).

Figure 3C shows the orientations of the planes selected with the FMSI and LSIB methods. The same nodal planes are chosen as fault planes for both methods. Yet the direction N210°E is not chosen as a slip direction whereas it was the most frequent one. This may mean that the nodal planes that have been selected as fault plane are those determined with the largest uncertainties.

Misfit estimators suggest the inversion is rather well resolved with each of the three methods. However, looking at the confidence regions we observe that only the minimal stress direction is well constrained and the only sure result for the other two directions is that they are in a plane perpendicular to σ3. According to Hardebeck and Hauksson (2001), the error domain of FMSI are too large. In our case, they are larger than LSIB's but principally at the 95% level. However it is difficult to compare the two of them because they are not calculated in the same way.

Breakout and Drilling Induced Tension Fractures (DITF) analysis were conducted in two deep boreholes (respectively 5000m and 2757m deep) in Basel (Valley and Evans (2009)). Figure 1 shows their location (BS1 and OT2). Valley and Evans found a principal stress oriented N151°E±13° from DTIF and N143°E±14° from breakout It makes a combined value with a weighted frequency of occurrence of N144°E±14°. All methods yield a maximal principal stress direction orientation more northernly than the N144°E value derived from the boreholes. The value derived with SSSCM is the most different one, but LSIB is within the error bars of the mean value. Plenefisch and Bonjer (1997) performed an inversion of focal mechanism in the southern Rhine Graben with Gephart and Forsyth (1984)'s method and they found a minimal principal direction oriented N69°E and a R value equal to 0.5. They performed several other inversions at different depth ranges and found that around 15km depth the regime changes from strike-slip to normal and the principal minimal direction rotates from N55°E to N65°E. Since the Sierentz earthquakes are located in the 9.5-14.5km depth range our solution is seen to be compatible with Plenefisch and Bonjer results.

The small difference in results obtained with FMSI and LSIB raises the question about the physics that underlines each method. One possibity is that the pore pressure is not constant within the domain that has been considered. Indeed after an earthquake, the pore pressure is known to be variable in space (Brodsky and al, 2003). Further, the fact that the SSSCM method yields a value more than 10° off the value derived from breakouts and DITF orientation suggest that the Tresca criterion is not very appropriate and that a Coulomb failure criterion is more satisfactory.

CONCLUSION

We have inverted focal mechanisms with three different methods. Each method taken separately yields satisfactory results but taken together they show a variability of at least 10° for the principal stress directions orientations. When looking at the error domain we find that only the minimum principal stress direction is well resolved.

BIBLIOGRAPHY

J. Angelier, 2002. Inversion of earthquake focal mechanisms to obtain the seismotectonic stress IV-a new method free of choice among nodal planes. Geophys. J. Int., 150, 588-609.

E. E. Brodsky, E. Roeloffs, D. Woodcok, I. Gall and M. Manga, 2003. A mechanism for sustained groundwater pressure changes induced by distant earthquakes. J. Geophys. Res., 108, 7,1-7,10.

J. W. Gephart and D. W. Forsyth, 1984. An improved method for determining regional stress tensor using earthquake focal mechanism data: application to the San Fernando earthquake sequence. J. Geophys. Res., 89, 9305-9320.

J. L. Hardebeck and E. Hauksson, 2001. Stress orientations obtained from earthquake focal mechanisms: what are appropriate uncertainty estimates? Bull. Seismol. Soc. Am. 91, 250-262.

Ph. Julien and F.H. Cornet, 1987. Stress determination from aftershocks of the Campania-Lucania earthquake of November 23, 1980. Ann. Geophys., 5B, 289-300.

A. J. Michael, 1984. Determination of stress from slip data: faults and folds. J. Geophys. Res., 89, 11,517-11,526.

A. J. Michael, 1987. Use of focal mechanisms to determine stress: a control study. J. Geophys. Res., 92, 357-368.

T. Plenefisch and K. Bonjer, 1997. The stress field in the Rhine Graben area inferred from earthquake focal mecanisms and estimation of frictional parameters. Tectonophysics, 275, 71-97.

D. Rouland, H. Haessler, K. P. Bonjer, B. Gilg, D. Mayer-Rosa and N. Pavoni, 1980. The Sierentz Southern-Rhine Graben earthquake of July 15, 1980. Preliminary results. Proc. of the 17th Ass. of the ESC Budapest.

B. Valley and K. F. Evans, 2009. Stress orientation to 5 km depth in the basement below Basel (Switzerland) from borehole failure analysis. Swiis J. Geosci.,